

Design of photonic crystal fibers for dispersion compensation over S, C and L bands

S. KONAR, RAKHI BHATTACHARYA

Department of Applied Physics, Birla Institute of Technology, Mesra- 835215, Ranchi, Jharkhand, India

We have investigated, index guided photonic crystal fibers that has eleven rings consisting of air holes. The dispersion characteristics, effective index, the fiber V parameter and field of the fundamental mode have been numerically investigated using the finite difference time domain (FDTD) method. These fibers show largest normal dispersion when air holes in all rings are of same diameter. Exhibited dispersion profile of the fiber has been flattened, albeit with significantly reduced value, by controlling the diameter of air holes in different outer and inner rings. It has been realized that smaller air holes in the first ring has the strongest influence in flattening the dispersion profile, however, it also significantly reduces the value of dispersion simultaneously which can be abated partially by introducing smaller air holes in outer rings. Investigated mode field profiles in all cases show that the fundamental modes are always confined within the fiber core. The proposed fiber may be useful in compensating for the dispersion over entire S, C and L bands.

(Received July 27, 2007; accepted August 31, 2007)

Keywords: Photonic crystal fibers, Dispersion compensation, FDTD method

1. Introduction

Optical fibers have diverse applications in telecommunications, medical instrumentations, sensors, fabrication of fiber optic based devices, soliton lasers etc. A conventional optical fiber usually relies on light being guided by total internal reflection (TIR), or index guiding. In order to achieve TIR, a core with higher refractive index compared to the surrounding media is required [1]. There are some limitations of conventional optical fibers, for example, conventional optical fibers exhibit very low normal dispersion that can be used for compensating the residual dispersion from 1510 to 1620 nm wavelength range in optical communication systems. In addition, optical nonlinearity in standard fiber is very small, an inevitable consequence is the inadvertently large fiber length for nonlinearity based devices. To overcome fundamental limitations of these conventional silica fibers, an alternate fiber, particularly, photonic crystal fiber, also known as microstructured fiber, was recently proposed [2-8]. A very important feature of PCF is that it can be made of single material in contrast to all other types of optical fibers, which are manufactured with two or more materials. The main difference between a microstructure optical fiber and a conventional optical fiber is that, microstructure optical fibers feature an air-silica cross-section, whereas, standard optical fibers have an all glass cross section. PCFs can exhibit unique dispersion characteristics, achieve very high birefringence, provide single mode operation over large wavelength range and can offer very large or low nonlinearity and can transport light with very low loss in certain wavelength range where conventional optical fibers are very lossy. In a PCF, air hole size, hole to hole distance provide additional degree of freedom in fiber design which facilitated a complete control on its

properties, such as ultra-flattened and high negative dispersion etc.

Chromatic dispersion is one of the most important issues encountered in long haul optical communication systems because of its strong influence on temporal pulse shape. Photonic crystal fibers have been contemplated for use in dispersion compensation since they exhibit large normal dispersion over optical communication wavelength. Several authors have investigated chromatic dispersion characteristics of PCFs [9-12]. In a recent investigation, Ni et. al. [13] has investigated dispersion performance of a dual-core PCF which exhibits a chromatic dispersion whose value is as large as $-18000 \text{ ps}/(\text{nm.km})$. However, the bandwidth over which the fiber exhibits large dispersion is only about 3 nm. In this paper, our goal is to design PCF with high normal dispersion parameter that can be employed for dispersion compensation over S (1480nm to 1525nm), C (1530 nm to 1565 nm) and L (1570 nm to 1610 nm) bands.

2. Design of the photonic crystal fibers

We have investigated an index guided PCF with a triangular lattice of air holes. A schematic of the fiber is shown in Fig. 1, which has eleven rings of circular air holes. A missing air hole at the center acts as the fiber core. The refractive index of air holes and fiber are 1 and 1.45 respectively. We have taken two different types of rings. In one type of ring, diameter of air holes is larger than that of the other type. All air holes in any individual ring possess equal diameter. The hole diameter of the i th ring is d_i , and the distance between centers of air holes i.e., hole pitch is Λ . Air hole diameter, hole pitch and refractive index of fiber materials determine the dispersive

property of the fiber. In addition, number of rings with small air holes and their location also play an important role in determining the dispersive property of the fiber and mode structure of optical fields as well. The mode field patterns of the fundamental mode and its chromatic dispersion properties have been investigated using well known on FDTD simulation [14]. The effective refractive index of the fundamental mode is given by

$$n_{eff} = \frac{\lambda}{2\pi} \beta, \text{ where } \lambda \text{ is the free space wavelength}$$

and β is the propagation constant. Once the modal effective index is known, the waveguide dispersion

$$\text{coefficient } D_w \text{ can be obtained as } D_w = -\frac{\lambda}{c} \frac{d^2 n_{eff}}{d\lambda^2},$$

where c is the velocity of light in vacuum. The total dispersion has been calculated as the sum of material dispersion and waveguide dispersion i.e., $D = D_m + D_w$, where the material dispersion can be directly obtained from Sellmeier equation [15].

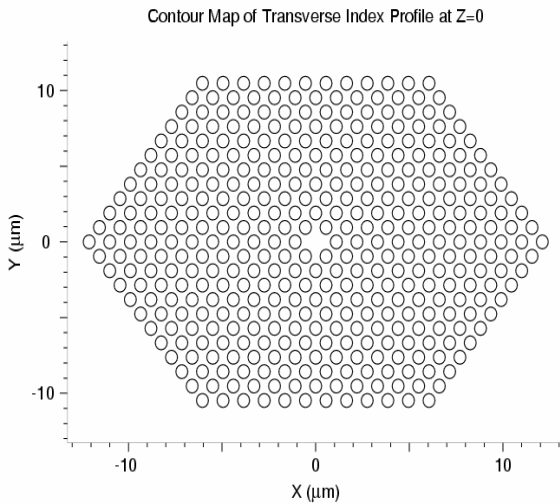


Fig. 1. Proposed eleven ring PCF with triangular lattice of air holes.

First we analyze the dispersion property of the PCF when all the rings possess air holes of same size. The hole diameter of each ring is $d = 0.65 \mu\text{m}$, hole pitch $\Lambda = 1.1 \mu\text{m}$ and core diameter $1.45 \mu\text{m}$. Fig. 2 shows the chromatic dispersion of the fundamental mode as a function of wavelength from 1400nm to 1700nm . Due to large refractive index difference between the core and effective cladding, the PCF exhibits a large normal dispersion of as much as $-1400 \text{ps} \cdot \text{nm}^{-1} \cdot \text{km}^{-1}$ at 1540nm with a large dispersion slope over 1450nm to 1650nm . It is evident from the figure that, in the C band (i.e., 1530nm to 1565nm) dispersion is larger than

$-1200 \text{ps}/(\text{nm} \cdot \text{km})$ and in the L band (1570nm to 1610nm) the dispersion varies between $-560 \text{ps}/(\text{nm} \cdot \text{km})$ to $-1200 \text{ps}/(\text{nm} \cdot \text{km})$. Similarly in the S band (1480nm to 1525nm), it varies between $-600 \text{ps}/(\text{nm} \cdot \text{km})$ to $-1200 \text{ps}/(\text{nm} \cdot \text{km})$. The bandwidth of large dispersion is about 130nm . The dispersion of the proposed fiber is at least five times larger than that of a conventional dispersion compensating fiber. For example, commercially available dispersion compensating fibers usually show a dispersion value as low as between $-100 \text{ps}/(\text{nm} \cdot \text{km})$ to $-150 \text{ps}/(\text{nm} \cdot \text{km})$ in the C band. Therefore, the proposed fiber can be used as a dispersion compensating fiber in the S, C and L bands.

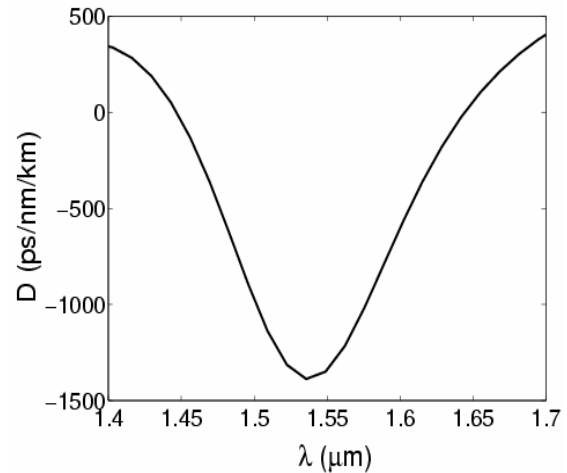


Fig. 2. Variation of total dispersion with λ for equal air hole diameter in all rings. $d_1 = d_2 = \dots = d_{11} = 0.75 \mu\text{m}$. $\Lambda = 1.1 \mu\text{m}$ and core diameter $1.45 \mu\text{m}$.

Effect of small air holes only in the outer rings: In the next stage of investigation, we replace outer rings with air holes of small diameter. We gradually increase the number of rings with small air holes in the outer region by one and investigate the dispersive property of the fiber. In each case, small air hole diameter has been fixed at $d = 0.255 \mu\text{m}$, while the diameter of each large air hole is $0.75 \mu\text{m}$. An increase in the number of rings with small air holes in the outer region will decrease the refractive index contrast. Therefore, the magnitude of normal dispersion is expected to decrease with the increase in the number of rings with small air holes in the outer region. Curves (b), (c), (d), and (e) of Fig. 3 represent chromatic dispersion of the fundamental mode respectively for one, two, three and four outer rings with small air holes. The dispersion profile of the fiber, when all rings consist of large air holes, has been also depicted in this figure by the curve (a) for the sake of comparison. From figure, it is amply clear that the introduction of

small air holes only in the outer region not only reduces the range of wavelength over which large normal dispersion is achievable but also decreases the value of dispersion. The effective refractive index n_{eff} of the fundamental mode has been depicted in Fig. 4. An important parameter associated with the crystal fiber is the effective V parameter defined as

$$V_{eff} = 2\pi \frac{\Lambda}{\lambda} \sqrt{n_{co}^2 - n_{eff}^2}, \text{ where } n_{co} \text{ is the core}$$

refractive index. The variation of V parameter with normalized wavelength has been depicted in Fig. 5. A careful examination of the variation of V parameter with λ/Λ shows that its value is always less than 4 signifying single mode operation over entire S, C and L bands covering 1480–1610 nm.

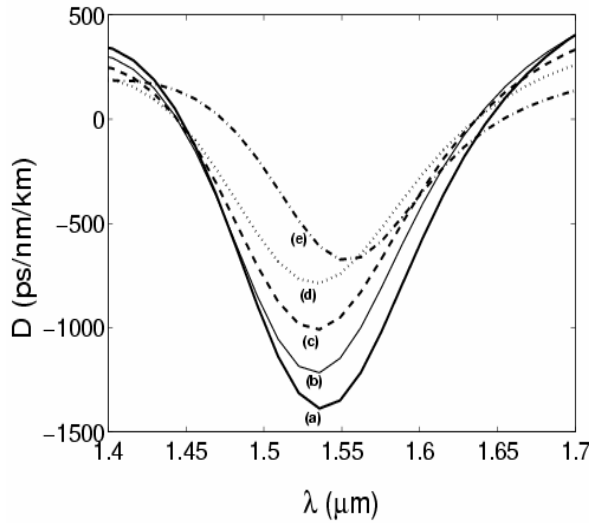


Fig. 3. Variation of total dispersion with λ for different number of outer rings with small air holes.

$\Lambda = 1.1 \mu\text{m}$. a) $d_1 = d_2 = \dots = d_{11} = 0.75 \mu\text{m}$,

(b) $d_1 = d_2 = \dots = d_{10} = 0.75 \mu\text{m}$, $d_{11} = 0.255 \mu\text{m}$,

(c) $d_1 = d_2 = \dots = d_9 = 0.75 \mu\text{m}$, $d_{10} = d_{11} = 0.255 \mu\text{m}$

(d) $d_1 = d_2 = \dots = d_8 = 0.75 \mu\text{m}$,

$d_9 = d_{10} = d_{11} = 0.255 \mu\text{m}$, and

(e) $d_1 = d_2 = \dots = d_7 = 0.75 \mu\text{m}$,

$d_8 = \dots = d_{11} = 0.255 \mu\text{m}$.

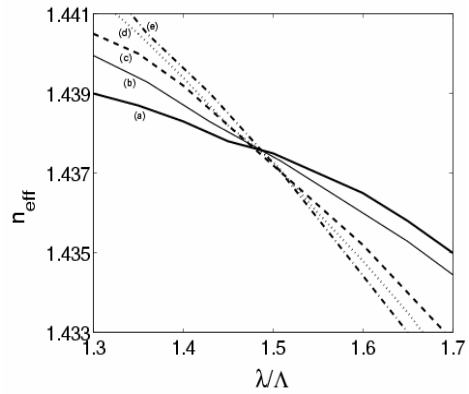


Fig. 4. Variation of n_{eff} of the fundamental mode of the fiber with λ/Λ for different number of outer rings with small air holes. $\Lambda = 1.1 \mu\text{m}$.

(a) $d_1 = d_2 = \dots = d_{11} = 0.75 \mu\text{m}$,

(b) $d_1 = d_2 = \dots = d_{10} = 0.75 \mu\text{m}$, $d_{11} = 0.255 \mu\text{m}$

(c) $d_1 = d_2 = \dots = d_9 = 0.75 \mu\text{m}$, $d_{10} = d_{11} = 0.255 \mu\text{m}$

(d) $d_1 = d_2 = \dots = d_8 = 0.75 \mu\text{m}$,

$d_9 = d_{10} = d_{11} = 0.255 \mu\text{m}$, and

(e) $d_1 = d_2 = \dots = d_7 = 0.75 \mu\text{m}$,

$d_8 = \dots = d_{11} = 0.255 \mu\text{m}$.

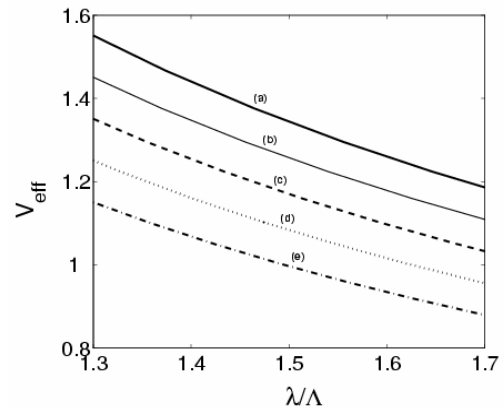


Fig. 5. Variation of V parameter of the fiber with λ/Λ for different number of outer rings with small air holes. $\Lambda = 1.1 \mu\text{m}$.

(a) $d_1 = d_2 = \dots = d_{11} = 0.75 \mu\text{m}$,

(b) $d_1 = d_2 = \dots = d_{10} = 0.75 \mu\text{m}$, $d_{11} = 0.255 \mu\text{m}$

(c) $d_1 = d_2 = \dots = d_9 = 0.75 \mu\text{m}$, $d_{10} = d_{11} = 0.255 \mu\text{m}$

(d) $d_1 = d_2 = \dots = d_8 = 0.75 \mu\text{m}$,

$d_9 = d_{10} = d_{11} = 0.255 \mu\text{m}$, and

(e) $d_1 = d_2 = \dots = d_7 = 0.75 \mu\text{m}$,

$d_8 = \dots = d_{11} = 0.255 \mu\text{m}$.

Effect of small air holes only in the innermost rings:

An interesting design aspect is to examine the effect of introducing small air holes only in the inner rings. Naturally, we should expect smaller chromatic dispersion due to reduced index contrast. In order to analyze this effect, we first design a fiber in which only the innermost ring possesses air holes with small diameter in comparison to other air holes. The fiber parameters are taken as follows: $d_1 = 0.60\mu\text{m}$, $d_2 = d_3 = d_4 = \dots = d_{11} = 0.75\mu\text{m}$, $\Lambda = 1.1\mu\text{m}$ and core size is $1.45\mu\text{m}$. The chromatic dispersion profile of the fundamental mode is shown in curve (a) of Fig. 6. It is evident that, in comparison to the dispersion characteristics of a fiber with equal air holes of size $d_i = 0.75\mu\text{m}$ in all rings, as expected the value of chromatic dispersion (normal) in the present case decreases very sharply between the wave length ranges 1480nm to 1610nm . However, the dispersion curve is comparatively flat with reduced dispersion slope. We have verified that further decrease of the value of d_1 , keeping outer holes unchanged, reduces dispersion slope, albeit with significant reduction of dispersion. We have increased the value of d_1 to $0.65\mu\text{m}$, keeping other parameters unchanged, and the dispersion profile for this case is labeled (b) in Fig. 6. The effect of increasing hole size is to enhance dispersion. Our next step is to design a fiber in which the second ring is with smaller holes having $d_2 = 0.65\mu\text{m}$, and the diameter of all other holes is of $0.75\mu\text{m}$. We have studied the dispersive property of this fiber, which is found to increase in the wavelength range between 1480nm to 1610nm , this has been displayed by curve (c) of Fig. (6). Still further improvement in the value of dispersion takes place when both first and second rings composed of air holes of smaller diameter and as an example curve (d) of Fig. (6) displays this, specifically for $d_1 = d_2 = 0.65\mu\text{m}$. An important worth noting feature is that the introduction of small air holes in the inner rings shifts the peak value of dispersion towards higher wavelength. Though these designs yield much lower normal dispersion in comparison to a fiber with all identical air holes, still they may be useful in certain applications where small dispersion slope is favorable. For example, the curve labeled (b), offers a dispersion whose value is approximately $-500\text{ps}/\text{nm.km}$ over wavelength range $1530\text{-}1565\text{nm}$ and $1570\text{-}1610\text{nm}$, and in both these wavelength bands dispersion slope is small comparison to other curve. The fiber corresponding to this curve may be preferred for use in dispersion compensation due to small dispersion slope that will yield low residual dispersion after the link.

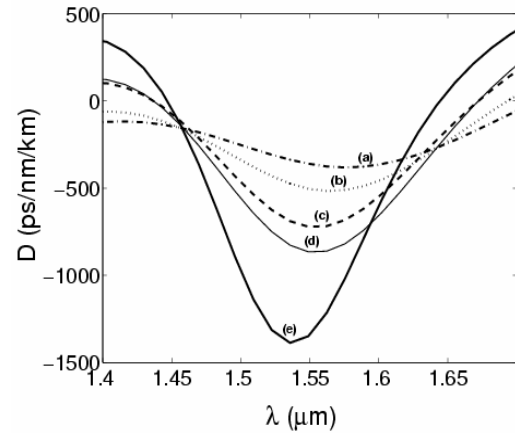


Fig. 6. Variation of total dispersion with λ when first ring, second ring or both of them possess air holes with small diameter. The hole pitch $\Lambda = 1.1\mu\text{m}$.

(a) $d_1 = 0.60\mu\text{m}$, $d_2 = \dots = d_{11} = 0.75\mu\text{m}$,

(b) $d_1 = 0.65\mu\text{m}$,

$d_2 = \dots = d_{11} = 0.75\mu\text{m}$,

(c) $d_2 = 0.65\mu\text{m}$,

$d_1 = d_3 = d_4 = \dots = d_{11} = 0.75\mu\text{m}$,

(d) $d_1 = d_2 = 0.65\mu\text{m}$, $d_3 = d_4 = \dots = d_{11} = 0.75\mu\text{m}$, and

(e) $d_1 = d_2 = \dots = d_{11} = 0.75\mu\text{m}$.

Effect of small air holes both in the inner and outer rings:

It can be shown that the dispersion profile of the fiber can be made comparatively flat with small value of dispersion slope by reducing the hole size of inner as well as outer rings. Therefore, in the next phase of the design, we replace both outer as well as inner rings with smaller air holes. The typical fiber is shown in Fig. 7. The dispersion profile of the fiber has been demonstrated in Fig. 8 when it consists of small air holes in two inner rings and variable number of outer rings as well. The air hole diameter of two inner rings has been kept at $d_1 = d_2 = 0.60\mu\text{m}$ and a variable number of outer rings possess air holes with diameter $d_i = 0.50\mu\text{m}$, while the diameter of other air holes has been kept constant at a value $d = 0.75\mu\text{m}$. The dispersion profiles of the fiber with two, three and four outer rings of small air holes have been demonstrated in figure (8). It is evident from the figure that introduction of small air holes both in the outer and inner rings shift the maximum dispersion achievable wavelength λ_{md} in the L band. The dispersion profile is comparatively flat, though the value of dispersion has reduced significantly. Nevertheless, in the L and C bands, available dispersion for compensation is always greater than $-500\text{ps}/\text{nm.km}$ when outer region consists of three or four rings with air holes of smaller diameter. Increasing the number of rings of small air holes in the outer region beyond four, though increases

the value of dispersion, is not helpful since the core cladding index contrast is not sufficient to confine the mode field in the central core region of the fiber. As a result such a fiber supports a fundamental mode that is ring shaped and lies outside the central core. A typical mode field of the fundamental mode has been demonstrated in Fig 9. The fiber dispersion characteristics may further be flattened by reducing the hole diameter of the two inner rings. Such a flat dispersion profile has been depicted in Fig. (10). It is evident that, for a wide bandwidth of about 300 nm, the fiber dispersion is approximately uniform, though the value is comparatively small.

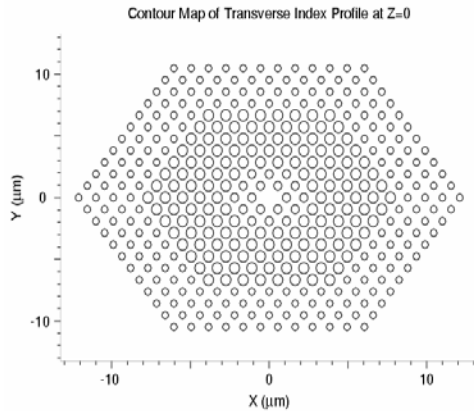


Fig. 7. Schematics of the crystal fiber with rings of small air holes in inner as well as outer regions.

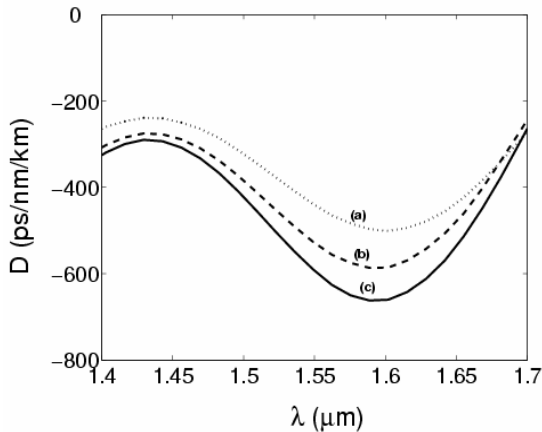


Fig. 8. Variation of total dispersion with λ of the crystal fiber with rings of small air holes in inner as well as outer regions. . The hole pitch $\Lambda = 1.1 \mu\text{m}$.

(a) $d_1 = d_2 = 0.60 \mu\text{m}$, $d_3 = \dots = d_9 = 0.75 \mu\text{m}$ and $d_{10} = d_{11} = 0.50 \mu\text{m}$, (b) $d_1 = d_2 = 0.60 \mu\text{m}$, $d_3 = \dots = d_8 = 0.75 \mu\text{m}$ and $d_9 = d_{10} = d_{11} = 0.50 \mu\text{m}$, (c) $d_1 = d_2 = 0.60 \mu\text{m}$, $d_3 = \dots = d_7 = 0.75 \mu\text{m}$ and $d_8 = d_9 = d_{10} = d_{11} = 0.50 \mu\text{m}$.

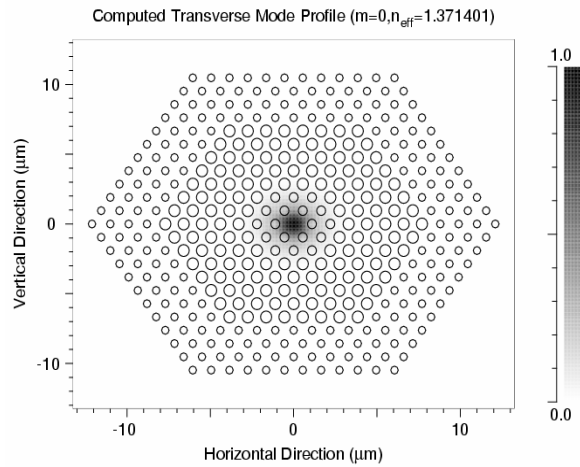


Fig. 9. A typical mode field pattern of proposed eleven-ring PCF with small air holes both in inner and outer rings $d_1 = d_2 = 0.60 \mu\text{m}$, $d_3 = \dots = d_7 = 0.75 \mu\text{m}$ and $d_8 = d_9 = d_{10} = d_{11} = 0.50 \mu\text{m}$.

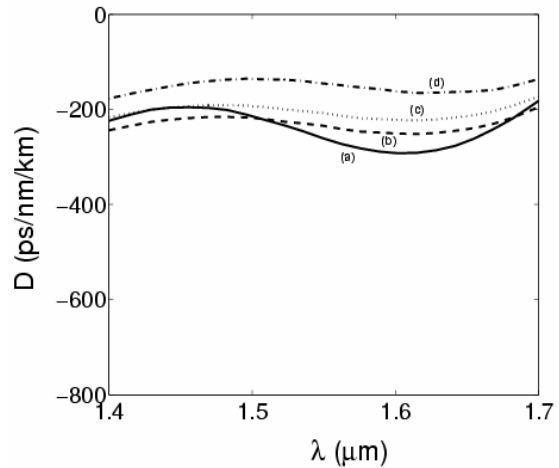


Fig. 10. Variation of total dispersion with λ of the crystal fiber with rings of small air holes in inner as well as outer regions. . The hole pitch $\Lambda = 1.1 \mu\text{m}$.

(a) $d_1 = d_2 = 0.45 \mu\text{m}$, $d_3 = \dots = d_9 = 0.75 \mu\text{m}$ and $d_{10} = d_{11} = 0.50 \mu\text{m}$.
 (b) $d_1 = d_2 = 0.42 \mu\text{m}$, $d_3 = \dots = d_8 = 0.75 \mu\text{m}$, $d_9 = d_{10} = d_{11} = 0.50 \mu\text{m}$.
 (c) $d_1 = d_2 = 0.40 \mu\text{m}$, $d_3 = \dots = d_7 = 0.75 \mu\text{m}$, $d_8 = d_9 = d_{10} = d_{11} = 0.50 \mu\text{m}$ and
 (d) $d_1 = d_2 = 0.36 \mu\text{m}$, $d_3 = \dots = d_7 = 0.75 \mu\text{m}$, $d_8 = d_9 = d_{10} = d_{11} = 0.50 \mu\text{m}$.

3. Conclusion

We have investigated the optical properties of an index guided microstructure fiber with triangular lattice of air holes. The dispersion characteristics, effective index, the fiber V parameter and mode field of the fundamental mode of the fiber have been numerically investigated using the FDTD method. The proposed fiber exhibits very large dispersion over the entire S, C and L bands. The exhibited dispersion profile has been flattened, albeit with significantly reduced value, by tailoring the hole size of inner and outer rings. The investigated mode field profiles in all cases show that the fundamental modes are always confined within the fiber core. The proposed fiber can compensate effectively for dispersion in the entire optical communication wavelength covering the S, C and L bands.

Acknowledgment

The Department of Science and Technology (DST), Government of India, support this work through the R&D grant SR/S2/LOP-10/2004. One of the authors, Rakhi Bhattacharya, would like to thank DST for providing a junior research fellowship.

References

- [1] A. Ghatak, K. Thyagarajan; Introduction to Fiber Optics, Cambridge University Press, (2002).
- [2] T. A. Birks, J. C. Knight, P. S. J. Russell; Opt. Lett. **22**, 961-963 (1997).
- [3] E. Silvestre, P. St. J. Russell, T. A. Birks, J. C. Knight; J. Opt. Soc. Am A **15**, 3067 (1998).
- [4] K. Saitoh, M. Koshiba; Optics Express **13**, 256 (2005).
- [5] Y. C. Liu, Y. Lai; Optics Express **13**, 225 (2005).
- [6] E. Knudsen, A. Bjarklev; Optics Communication **222**, 155 (2003).
- [7] T. P. Hansen, J. Broeng, E. B. Libori, E. Knudsen, A. Bjarklev, J. R. Jensen, H. Simonsen; IEEE Photon. Tech. Lett. **13**, 588-590 (2001).
- [14] J. C. Knight, T. A. Birks, P. St. J. Russell, D. M. Atkim; Opt. Letts. **21**, 1547 (1996).
- [15] T. A. Birks, D. Mogilevstev, J. C. Knight, P. S. J. Russell; IEEE Photon. Tech. Lett. **11**, 674-676 (1999).
- [16] L. P. Shen, W. P. Huang, G. X. Chen, S. S. Jian; IEEE Photon. Tech. Lett. **15**, 540-542 (2003).
- [17] F. Grme, J. Auguste, J. Blondy; Opt. Letts. **29**, 2725 (2004).
- [18] X. Yu, P. Shum; J. Optoelectron. Adv. Mater. **7**, 3185 (2005).
- [19] Y. Ni, L. An, J. Peng, C. Fan; IEEE Photon. Tech. Lett. **16**, 1516 (2004).
- [20] BandSOLVE™ 1.3; RSoft Design Group Inc., Ossining, (NY) (2003).
- [21] G. Agrawal, Nonlinear Fiber Optics. New York: Academic, (1995).

*Corresponding author: swakonar@yahoo.com